Received: 1 May 2016 | Revised: 11 July 2016 | Accepted: 14 July 2016

DOI 10.1002/aoc.3583

WILEY Applied Organometallic Chemistry

FULL PAPER

New bioactive Pt(II) binary and ternary metal complexes with guaifenesin drug: Synthesis, geometrical structure, and spectroscopic and thermal characterization

Walaa H. Mahmoud | Gehad G. Mohamed* | Nessma F. Mahmoud

Chemistry Department, Faculty of Science, Cairo University, Giza 12613, Egypt

Correspondence
Gehad G. Mohamed, Chemistry Department, Faculty of Science, Cairo University, Giza, 12613, Egypt.
Email: ggenidymohamed@sci.cu.edu.eg

Three new binary and ternary metal complexes of Pt(II) with guaifenesin (GFS) drug have been prepared by chelation to guaifenesin ligand (as primary ligand) and glycine amino acid (HGly) and 1,10-phenanthroline (1,10-Phen) (as secondary ligands). Characterization was conducted based on elemental analysis, molar conductance, infrared (IR) spectroscopy, thermogravimetric analysis and X-ray diffraction. The complexes were found to have the formulae $[Pt(GFS)_2]\cdot 3H_2O$ (**1**), $[Pt(GFS)_2(Gly)]Cl\cdot H_2O$ (**2**) and $[Pt(GFS)_2(Phen)]Cl_2$ (**3**). Magnetic and spectroscopic data revealed complexes **1–3** to have octahedral geometry. IR spectra suggested that GFS ligand coordinated in mononegative tridentate mode (OOO) for **1** but in neutral bidentate mode (OO) for **2** and **3**. In addition, HGly behaves as mononegative bidentate coordinated to Pt(II) metal via deprotonated carboxylate O and amino group. IR data also evidenced the bidentate nature of 1,10-Phen ligand. The molecular and electronic structure of Pt(II) complex **1** was optimized theoretically and the quantum chemical parameters were calculated. Complexes **1–3** were screened for their antibacterial activity on Gram-positive bacteria (*Bacillus subtilis* and *Staphylococcus aureus*) and Gram-negative bacteria (*Escherichia coli* and *Neisseria gonorrhoeae*) and for their *in vitro* antifungal activity against *Candida albicans*. The three Pt(II) complexes showed remarkable biological and cytotoxic activity. The chelates were also screened for their *in vitro* anticancer activity against the MFC7 breast cell line. Complex **3** showed the highest activity with a low IC_{50} value of 3.38 μg ml^{-1}.

KEYWORDS

activity index, biological and anticancer activity, molecular structures, Pt(II) chelates, quantum chemical parameters, spectroscopy, thermal analyses

1 | INTRODUCTION

Metal complexes have many characteristics that can be advantageous in drug design. Transition metals have an important place in medicinal biochemistry. Research has made significant progress in utilization of transition metal complexes as drugs to treat several human diseases like carcinomas, lymphomas, infections, diabetes, inflammation and neurological disorders. The medicinal uses and applications of metals and metal complexes are of increasing clinical and commercial importance.[1] There has been an increased interest in the last few decades in the use of metal ions and complexes as chemotherapeutic agents. Emphasis has been placed mainly on cancer treatment, as a result of the great success of cisplatin and new-generation analogous platinum compounds. The development of medicinal inorganic chemistry has been supported by the advances in bioinorganic chemistry, as can be evidenced in recent reviews including several applications of a variety of metal complexes in medicine, as well as the chemistry and biochemistry involved.[2] A significantly rising interest in the design of metal compounds as drugs and diagnostic agents is currently observed in the area of scientific inquiry

that is termed medicinal inorganic chemistry. Investigations in this area have focused mostly on the speciation of metal species in biological media based on possible interactions of these metal ions with diverse biomolecules, in an effort to contribute to future development of new therapeutics or diagnostic agents. Metallopharmaceuticals used as anticancer agents, metal-mediated antibiotics, antibacterials, antivirals, antiparasitics, antiarthritics, antidiabetics and radio-sensitizing agents have appeared in therapeutic medicinal inorganic chemistry. The medicinal uses and applications of metals and metal complexes are of increasing clinical and commercial importance.[3]

There has been a rapid expansion in research and development of new metal-based anticancer drugs to improve clinical effectiveness, reduce general toxicity and broaden the spectrum of activity. Chemical, pharmacological and clinical research on anticancer coordination complexes has yielded remarkable anticancer agents such as cisplatin, carboplatin and oxaliplatin. Cisplatin is regarded as one of the most effective anticancer drugs, even if severe toxicities and drug resistance phenomena limit its clinical use. Among extensive research aiming to characterize other anticancer-active inorganic complexes with improved pharmacological properties compared to cisplatin is that focusing on the use of biologically active complexes formed by essential ions such as transition metals. Complexes with biologically active ligands are particularly attractive, as they combine qualities of classic non-targeted coordination compounds and organic ligands with selectivity for cellular targets.[4] Studies of such complexes are expected to indicate that new mechanisms of action are possible through combining the bioactivity of a ligand with the properties inherent to a metal, leading to the possibility of overcoming current drug resistance pathways.[5,6] Guaifenesin (International Nonproprietary Name; Figure 1) or guaiphenesin (former British Approved Name) is an expectorant drug usually taken orally to assist the expectoration ('bringing up') of phlegm from the airways in acute respiratory tract infections. It is a common ingredient in many over-the-counter cough/cold medications and its IUPAC name is 3-(2-methoxyphenoxy)propane-1,2-diol.[7] Guaifenesin works by thinning and loosening mucus in the airways, clearing congestion and making breathing easier. The principal use of guaifenesin is in the treatment of coughing. Guaifenesin is sometimes combined with dextromethorphan, an antitussive, such as in Mucinex DM or Robitussin DM,[8] or combined with, for example, propofol, since guaifenesin does not produce analgesia nor does it produce unconsciousness. Guaifenesin is a centrally acting muscle relaxant used routinely in large-animal veterinary surgery.

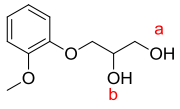

FIGURE 1 Structure of guaifenesin

This medication is used for the temporary relief of coughs caused by the common cold, bronchitis and other breathing illnesses. This product is usually not used for ongoing cough from smoking or long-term breathing problems (such as chronic bronchitis and emphysema) unless directed by a doctor.[9,10]

This paper described the characterization of guaifenesin drug (GFS) and its Pt(II) complexes $[Pt(GFS)_2]\cdot 3H_2O$ (**1**), $[Pt(GFS)_2(Gly)]Cl\cdot H_2O$ (**2**) and $[Pt(GFS)_2(Phen)]Cl_2$ (**3**) using elemental analyses, infrared (IR), ^1H NMR, mass and UV–visible spectroscopies, X-ray diffraction (XRD), magnetic moment, molar conductance and thermal analysis. The antimicrobial activities of GFS and its binary and ternary Pt (II) complexes **1**–**3** were studied and comparison of their antimicrobial activities with those of standard antibacterial and antifungal drugs was carried out. The molecular structure of Pt(II) complex **1** was studied and quantum chemical parameters were calculated. Moreover, the anticancer activity against the MCF7 breast cell line was studied.

2 | EXPERIMENTAL

2.1 | Materials and reagents

All chemicals used were of analytical reagent grade, and of highest purity available. The chemicals used included GFS drug which was supplied by the National Organization for Drug Control and Research, $PtCl_2$ and 1,10-phenanthroline (Merck) and glycine (BDH, Poole, UK). Organic solvents were spectroscopically pure from BDH including ethanol, diethyl ether and dimethylformamide (DMF). Hydrogen peroxide, sodium chloride, sodium carbonate and sodium hydroxide were used. Human tumour cell line (breast cell) was obtained frozen in liquid nitrogen (−180°C) from the American Type Culture Collection. The tumour cell line (MCF7) was maintained in the National Cancer Institute, Cairo, Egypt, by serial sub-culturing.

2.2 | Solutions

A fresh stock solution of 1×10^{-3} M of GFS (0.4 g l^{-1}) was prepared in the appropriate volume of absolute ethanol and DMF in a ratio of 1:3 (*v*/v). Dimethylsulfoxide (DMSO; Sigma Chemical Co., St Louis, MO, USA) was used in cryopreservation of cells. RPMI-1640 medium (Sigma) was used for culturing and maintenance of the human tumour cell lines. The medium was supplied in a powder form. It was prepared as follows: 10.4 g of medium was weighed, mixed with 2 g of sodium bicarbonate, completed to 1 l with distilled water and shaken carefully until complete dissolution. The medium was then sterilized by filtration with a Millipore bacterial filter (0.22 μm). The prepared medium was kept in a refrigerator (4°C) and checked at regular intervals for contamination. Before use the medium was warmed at 37°C in a water bath

and supplemented with penicillin/streptomycin and foetal bovine serum (FBS).

Sodium bicarbonate (Sigma) was used for the preparation of RPMI-1640 medium. Isotonic trypan blue solution (0.05%; Sigma) was prepared in normal saline and was used for viability counting. FBS (10%; heat-inactivated at 56°C for 30 min), 100 U ml^{-1} penicillin and 2 mg ml^{-1} streptomycin (Sigma) were used for the supplementation of RPMI-1640 medium prior to use. Trypsin (0.025% (*w*/*v*); Sigma) was used for the harvesting of cells. Acetic acid (1% (*v*/v); Sigma) was used for dissolving unbound sulphorhodamine-B (SRB) dye (0.4%; Sigma). A stock solution of trichloroacetic acid (50%; Sigma) was prepared and stored. An amount of 50 µl of the stock was added to 200 µl of RPMI-1640 medium per well to yield a final concentration of 10% used for protein precipitation. Isopropanol (100%) and ethanol (70%) were used. Tris base (10 mMl pH = 10.5) was used for SRB dye solubilization. An amount of 121.1 g of Tris base was dissolved in 1000 ml of distilled water and the pH was adjusted using hydrochloric acid (2 M).

Microanalyses of carbon, hydrogen and nitrogen were carried out at the Microanalytical Center, Cairo University, Egypt, using a CHNS-932 (LECO) Vario elemental analyser. IR spectra were recorded with a PerkinElmer 1650 spectrometer (400–4000 cm^{-1}) in KBr pellets. Electronic spectra were recorded at room temperature with a Shimadzu 3101pc spectrophotometer as solutions in ethanol. ^{1}H NMR spectra, as solutions in DMSO-d_6, were recorded with a 300 MHz Varian-Oxford Mercury at room temperature using tetramethylsilane as an internal standard. Electron spin resonance spectra were recorded with a JES-FE2XG ESR spectrophotometer at the Microanalytical Center, Tanta University. Mass spectra were recorded using the EI technique at 70 eV with a Hewlett-Packard MS-5988 GS-MS instrument at the Microanalytical Center, National Center for Research, Egypt. The molar magnetic susceptibility was measured on powdered samples using the Faraday method. The diamagnetic corrections were made by Pascal's constant and $Hg[Co(SCN)_4]$ was used as a calibrant. Molar conductivities of 10^{-3} M solutions of solid complexes in DMF were measured using a Jenway 4010 conductivity meter. Thermogravimetric analyses (TG and DTG) of the solid complexes were carried out from room temperature to 800°C using a Shimadzu TG-50H thermal analyser. Powder XRD analyses were carried out using a Philips Analytical X-Ray BV diffractometer type PW 1840. Radiation was provided by copper target (Cu anode, 2000 W) high-intensity X-ray tube operated at 40 kV and 25 mA. Divergence and the receiving slits were 1 and 0.2, respectively. The anticancer activity experiments were performed at the National Cancer Institute, Cancer Biology Department, Pharmacology Department, Cairo University. The optical density (OD) of each well was measured spectrophotometrically at 564 nm with an ELIZA microplate reader (Meter Tech, USA).

The molecular structure of Pt(II) complex **1** was optimized using the HF method with 3-21G basis set. The molecules were built with PerkinElmer ChemBio Draw and optimized using PerkinElmer ChemBio3D software.[11,12] Quantum chemical parameters such as the highest occupied molecular orbital energy (E_{HOMO}), the lowest unoccupied molecular orbital energy (E_{LUMO}) and HOMO–LUMO energy gap (ΔE) were calculated.

2.3 | Preparation of metal complexes

The binary metal complexes were prepared by the addition of a hot solution (70°C) of the appropriate metal chloride (1.07 mmol) in an ethanol–DMF mixture (1:3 *v*/v) to a hot solution (70°C) of the ligand (0.4 g of GFS, 2.02 mmol) in the same solvent (20 ml) and ethanolic ammonia solution was added to adjust the pH of the solution. The ternary metal complexes were prepared by the addition of a hot solution (70°C) of the metal chloride (2.02 mmol) in an ethanol–DMF mixture (1:3 v/v) to a hot solution (70°C) of the ligands (0.4 g of GFS, 0.149 g of glycine and 0.4 g of 1,10-phenanthroline, 2.02 mmol) in the same solvent (25 ml of each ligand) and ethanolic ammonia solution was added to adjust the pH of the solution. The resulting mixture was stirred under reflux for 1.5 h, whereupon the complexes precipitated. They were removed by filtration, washed with hot ethanol followed by diethyl ether and dried in a vacuum desiccator over anhydrous calcium chloride. The analytical data for C, H and N were obtained in duplicate. The solid complexes were then dried in a desiccator over anhydrous calcium chloride. The yield ranged from 60 to 80%.

Complex **1**. Dark brown; yield 66%; m.p. 156°C. Anal. Calcd (%): C, 38.62; H, 5.36; Pt, 30.22. Found (%): C, 38.54; H, 5.23; Pt, 30.32. μ_{eff} (BM): 3.36. Λ_m (Ω^{-1} mol^{-1} cm^2): 19.20. IR (cm^{-1}): ν(OH) stretching (CH_2—OH^a) 3251br; ν(OH) stretching (CH_2—OH^b) 3071 s; ν(C—O—C^b) etheric phenoxy stretching 1252sh; $\nu(CH_3O)$ methoxy 1224s; ν(CH—C—O^b) etheric 1180 m; ν(M—O) stretching bands of coordinated water 543 s; ν(M—O) stretching (OH, C—O) 650, 666. λ_{max} (nm): 273 π–π*. ^{1}H NMR (δ, ppm): 6.81–7.03 (m, 6H, Ar—H), band due to CH—OH^b disappeared, 4.60 (t, 1H, CH_2—OH^a, J = 2.7 Hz), 3.96 (d, 2H, O—CH_2, J = 1.8 Hz), 3.91 (m, 1H, CH—OH^b), 3.72 (s, 3H, O—CH_3), 3.47 (t, 2H, CH_2—OH^a, J = 2.4 Hz).

Complex **2**. Yellowish white; yield 80%; m.p. 80°C. Anal. Calcd (%): C, 36.70; H, 4.70; N, 1.90; Pt, 27.37. Found (%): C, 36.60; H, 4.60; N, 1.70; Pt, 27.96. μ_{eff} (BM): 3.32. Λ_m (Ω^{-1} mol^{-1} cm^2): 62.0. IR (cm^{-1}): ν(OH) stretching (CH_2—OH^a) 3239br; ν(OH) stretching (CH_2—OH^b) 3074 s; $\nu(NH_2)_{asym}$ 3120 s; $\nu(COO)_{asym}$ 1507sh; $\nu(COO)_{sym}$ 1461sh; ν(C—O—C^b) etheric phenoxy stretching 1251 m; $\nu(CH_3O)$ methoxy 1223sh; ν(CH—C—O^b) etheric 1183 m; $\nu(NH_2)$ bending 671 m; ν(M—O) stretching (OH, C—O) 635 m, 511 m; ν(M—N) 445 m. λ_{max} (nm): 272 π–π*.

Complex **3**. Orange; yield 60%; m.p. 60°C. Anal. Calcd (%): C, 45.60; H, 4.30; N, 3.30; Pt, 23.20. Found (%): C, 45.43; H, 2.99; N, 2.99; Pt, 25.0. μ_{eff} (BM): 3.27. Λ_m (Ω^{-1} mol^{-1} cm^2): 107.0. IR (cm^{-1}): ν(OH) stretching (CH_2—OH^a) 3228br; ν(OH) stretching (CH_2—OH^b) 3101 s; ν(C═N) stretching 1592sh; ν(C—O—C^b) etheric phenoxy stretching 1252 m; $\nu(CH_3O)$ methoxy 1223 m; ν(CH—C—O^b) etheric 1183 m; ν(pyridine ring) stretching 1125sh; ν(M—O) stretching (OH, C—O) 535 m, 500 s; ν(M—N) 417 s. λ_{max} (nm): 271 π–π*.

2.4 | Spectrophotometric studies

The absorption spectra of GFS free ligand and its Pt(II) complexes under study were scanned within the wavelength range from 200 to 700 nm.

2.5 | Antimicrobial activity

The *in vitro* antibacterial and antifungal activity tests were performed through the well diffusion method[13] using amikacin and ketokonazole as positive controls for bacteria and fungi, respectively. The bacteria used were *Bacillus subtilis*, *Staphylococcus aureus* (Gram-positive bacteria), *Escherichia coli* and *Neisseria gonorrhoeae* (Gram-negative bacteria). The fungus used was *Candida albicans*. Stock solution (0.001 mol) was prepared by dissolving the compounds in DMSO. The diameter of the inhibition zones was measured in millimetres. Measurements were performed in triplicate and the average was taken as the final reading.[14]

2.6 | Anticancer activity

Potential cytotoxicity of the compounds was tested using the method of Skehan and Storeng.[15] Cells were plated in a 96-multiwell plate (104 cells per well) for 24 h before treatment with the compounds to allow attachment of cells to the walls of the plate. Various concentrations of the compounds under investigation (0, 5, 12.5, 25, 50 and 100 μg ml^{-1}) were added to the cell monolayer and triplicate wells were prepared for each individual dose. The monolayer cells were incubated with the compounds for 48 h at 37°C and in 5% CO_2 atmosphere. After 48 h, cells were fixed, washed and stained with SRB stain. Excess stain was washed with acetic acid and attached stain was recovered with Tris–EDTA buffer. The OD of each well was measured spectrophotometrically at 564 nm with an ELIZA microplate reader and the mean background absorbance was automatically subtracted and mean values of each drug concentration were calculated. The relation between surviving fraction and drug concentration was plotted to get the survival curve of breast tumour cell line for each compound.

The percentage cell survival was calculated as follows:

$$\text{Survival fraction} = \frac{\text{OD (treated cells)}}{\text{OD (control cells)}}$$

The IC_{50} values (the concentrations of the GFS, HGly, 1,10-Phen or Pt(II) complexes required to produce 50% inhibition of cell growth) were obtained. The experiment was repeated three times.

3 | RESULTS AND DISCUSSION

The binary and ternary Pt(II) metal ion complexes with GFS ligand were synthesized as previously described and characterized by using physical and analytical techniques. IR spectral studies were used to infer the possible coordination sites of the ligands (GFS, HGly and 1,10-Phen) involved in binding to the metal ions. The synthesized complexes are dark brown, yellowish white and orange in colour and possess moderate melting points. These complexes are soluble in DMSO and DMF, slightly soluble in ethanol, but insoluble in water and other organic solvents. The suggested formula structures of the complexes are based on the results of molar conductivity measurements, mass, UV–visible and ^{1}H NMR spectra and powder XRD. In addition, the thermal analyses (TG and DTA) were used to confirm the suggested fragmentation patterns, the molecular formula of the chelates to differentiate between coordinated and hydrated water molecules and to determine the decomposition temperatures of the chelates. In addition, the biological activities of the ligands (GFS, HGly and 1,10-Phen) and their metal chelates were screened against various fungal and bacterial organisms. The complexes were also screened for their *in vitro* anticancer activity against the MFC7 cell line and the results obtained throw more light on the activity of these complexes.

3.1 | Elemental analysis and molar conductivity of complexes

The elemental analysis data of the complexes show the formation of the binary Pt(II) complex (complex **1**) in the ratio 1:2 (Pt(II):GFS) and correspond to a composition of [Pt $(GFS)_2]\cdot 3H_2O$. The colour of the binary complex is dark brown and its molar conductivity value is found to be 19.20 Ω^{-1} mol^{-1} cm^2, indicating its non-electrolytic nature.[16]

The ternary Pt(II) complexes with GFS and glycine amino acid (complex **2**) or 1,10-phenanthroline (complex **3**) are yellowish white and orange in colour, respectively. The molar conductivity values of the ternary Pt(II) metal complexes are found to be 62.0 and 107.0 Ω^{-1} mol^{-1} cm^2 for **2** and **3**, respectively, which indicate their electrolytic nature.[17]

3.2 | IR spectra

The characteristic IR vibrational frequencies of the free GFS ligand and its binary and ternary Pt(II) metal complexes were determined. The IR spectrum of GFS drug exhibits a band at 3246 cm^{-1} which can be attributed to alcoholic (—CH_2—OH^a) group. This band is still broad in the spectra of all complexes and appears at 3251, 3239 and 3228 cm^{-1} for complexes **1**, **2** and **3**, respectively. The band appears at about the same region for the three metal complexes thus confirming the non-involvement of the hydroxyl function (—CH_2—OH^a) in coordination with the metal ions. The shift can also be attributed to either hydrogen bond formation or the presence of hydrated and coordinated water molecules. The ν(OH) stretching vibration band due to alcoholic (—CH_2—OH^b) group appears in the spectrum of the free GFS ligand at 3078 cm^{-1}. For metal complex **1**, this band is shifted to lower wavenumber (3071 cm^{-1}) indicating the involvement of this group in complex formation. The CH—CO^b stretching vibration found for the free GFS ligand at 1183 cm^{-1} is shifted to lower wave number (1180 cm^{-1}) which supports coordination of CH_2—OH^b to metal ion or its involvement in bond formation. The band shift indicates the formation of a covalent bond between Pt(II) ion and this hydroxyl oxygen atom (CH—CO^b) after deprotonation in the binary Pt(II) complexes and hence confirms its binding to Pt(II) ion. This is further confirmed by ^{1}H NMR studies. For complexes **2** and **3**, the CH—C—O^b stretching vibration band appears in the same position (1183 cm^{-1}) indicating its non-participation in complex formation. This is also confirmed by the elemental and conductance data for complexes **2** and **3** due to the presence of anions in the outer coordination sphere.

Also, two absorption bands due to etheric C—O—C phenoxy and methoxy groups appear at 1255 and 1227 cm^{-1}, respectively, in the spectrum of free GFS ligand. The absorption frequencies of etheric C—O—C phenoxy in metal complexes **1**, **2** and **3** are shifted and appear at 1252, 1251 and 1252 cm^{-1}, respectively, indicating the involvement of oxygen atom of etheric C—O—C phenoxy in complexation with the metal ions.[18–21] For complexes **1**–**3**, the band due to methoxy oxygen atom (CH_3—O) is shifted to lower wavenumber upon chelation with Pt(II) ion indicating its binding to Pt(II) ion and hence the CH_3—O methoxy is involved in chelation.

The ν_{asym}(COO) and ν_{sym}(COO) stretching vibrations are observed at 1586 and 1412 cm^{-1}, respectively, for HGly free ligand.[21–24] Coordination with Pt(II) ion via the carboxylate O atom is indicated by the shift in position of the ν_{asym}(COO) and ν_{sym}(COO) stretching vibration bands to 1592 and 1460 cm^{-1}, respectively, for Pt(II) complex **2**. In the 3120 cm^{-1} region of the IR spectrum of complex **2** the $\nu(NH_2)$ stretching vibration is observed, which appears at 3400 cm^{-1} for the free HGly ligand, and the overlap of the various $\nu(NH_2)$ vibrations couple in many cases with water molecules of hydration or coordination which give rise to strong absorption. This makes it difficult to recognize individually the various bands appearing in this region. The bands due to the in-plane and out-of-plane bending of the amino group of HGly at 1524 and 760 cm^{-1}, respectively, can help in confirming the participation of the amino group of HGly in chelate formation. The $\delta(NH_2)$ in-plane and out-of-plane bending vibrations appear at 1507 and 784 cm^{-1} in Pt(II) complex **2** confirming the coordination of the amino group to the Pt(II) ion.[25]

The bands arising due to ν(C═N) stretching vibration and in-plane bending appear at 1588 and 625 cm^{-1}, respectively, in the spectrum of the 1,10-Phen ligand. In the ternary metal complex **3**, these bands are observed at 1592 and 624 cm^{-1}, respectively, indicating the involvement of nitrogen of pyridine ring in complex formation.[21,24–30]

The IR spectra of the three complexes each show a new band which is assignable to ν(M—O) stretching vibration at 543, 511 and 500 cm^{-1} for complexes **1**, **2** and **3**, respectively.[31,32] The ν(M—N) stretching vibrations appear at 445 and 417 cm^{-1} for complexes **2** and **3**, respectively.

Therefore, it is concluded from the IR spectra of binary and ternary metal complexes that:

1. For complex **1**, GFS behaves as a uni-negative tridentate ligand coordinated to Pt(II) ion via the etheric C—O—C phenoxy oxygen, methoxy oxygen and deprotonated hydroxyl oxygen (CH—OH^b). But, in the ternary complexes **2** and **3**, it behaves as neutral bidentate ligand coordinated to the metal ions via etheric C—O—C phenoxy and methoxy oxygen atoms.
2. For complex **2**, Gly behaves as a uni-negative bidentate ligand with NO donor sites and coordinated to the Pt (II) ion via the amino group N and deprotonated carboxylic oxygen.
3. For complex **3**, 1,10-Phen behaves as neutral bidentate ligand coordinated to the metal ion through two pyridine N atoms.

3.3 | ^{1}H NMR spectra

The ^{1}H NMR spectral data for GFS and its Pt(II) chelate **1** are discussed. It is found that the uncoordinated GFS has the respective peak positions and corresponding assignments: multiplet peak at 6.85–7.0 ppm (m, 6H, Ar—H) which corresponds to benzene ring; doublet peak occurs at 4.85 ppm (d, 1H, CH—O*H*^{b}) which is attributed to OH^b hydroxyl group; and triplet peak occurs at 4.61 ppm (t, 1H, CH_2—O*H*^{a}) which is attributed to OH^a hydroxyl group. In addition, doublet peak occurs at 3.98 ppm (d, 2H, O—CH_2) which is attributed to O—CH_2 methylene group, multiplet peak occurs at 3.94 ppm (m, 1H, C*H*—OH^b) corresponding to CH—OH^b methyne group, singlet peak occurs at 3.74 ppm (s, 3H, O—CH_3) which is attributed to methoxy group and triplet peak occurs at 3.48 ppm (t, 2H, CH_2—OH^a)

which is attributed to CH_2—OH^a methylene group.[19,20,33] For Pt(II) complex **1**, all the NMR peaks remain almost unaltered except that the peak corresponding to OH^b hydroxyl group disappears indicating its involvement in complex formation.

Due to the difficulties in solubility of complexes **2** and **3** in DMSO-d_6 solvent, the elemental analysis and IR spectral tools help in structural interpretation of the complexes.

3.4 | UV–visible spectra

Absorption spectra of the binary and ternary GFS–Pt(II) metal complexes **1**–**3** were obtained in DMF and ethanol (3:1 *v*/v) at room temperature. UV–visible spectra were recorded for these complex solutions (1×10^{-4} M) in the range 200–700 nm. The bands due to n–π* and π–π* transitions of the ligand are shifted to higher wavelengths in UV–visible spectra of the complexes. It is observed that free GFS has two distinct absorption bands. The first one at 223 nm may be attributed to π–π* transition of the benzene ring. The second band observed at 273 nm can be attributed to n–π* electronic transition.[19,20] In the spectra of complexes **1**, **2** and **3**, the band at 223 nm disappears while the one at 273 nm is observed at 273, 272 and 271 nm, respectively, indicating that the ligand is coordinated to metal ion.[19,20,29,34]

3.5 | Molecular structures

The optimized structure of Pt(II) complex **1** is shown in Figure 2. Selected geometric parameters, namely bond lengths and bond angles, of Pt(II) complex **1** are given in Table 1. The HOMO and LUMO of Pt(II) complex **1** are shown in Figure 3. The HOMO–LUMO energy gap, ΔE, which is an important stability index, was applied to develop theoretical models for explaining the structure and conformation barriers in many molecular systems.[28,35] The calculated quantum chemical parameters are given in Table 2. Additional parameters such as ΔE, absolute electronegativities, χ, chemical potentials, Pi, absolute hardness, η, absolute softness, σ, global electrophilicity, ω, global softness, S, and additional electronic charge, ΔN_{max}, have been calculated according to the following equations:

$$\Delta E = E_{LUMO} - E_{HOMO} \tag{1}$$

$$\chi = -\frac{E_{HOMO} + E_{LUMO}}{2} \tag{2}$$

$$\eta = \frac{E_{LUMO} - E_{HOMO}}{2} \tag{3}$$

$$\sigma - \frac{1}{\eta} \tag{4}$$

$$Pi = -\chi \tag{5}$$

$$S = \frac{1}{2\eta} \tag{6}$$

$$\omega = \frac{Pi^2}{2\eta} \tag{7}$$

$$\Delta N_{max} = -\frac{Pi}{\eta} \tag{8}$$

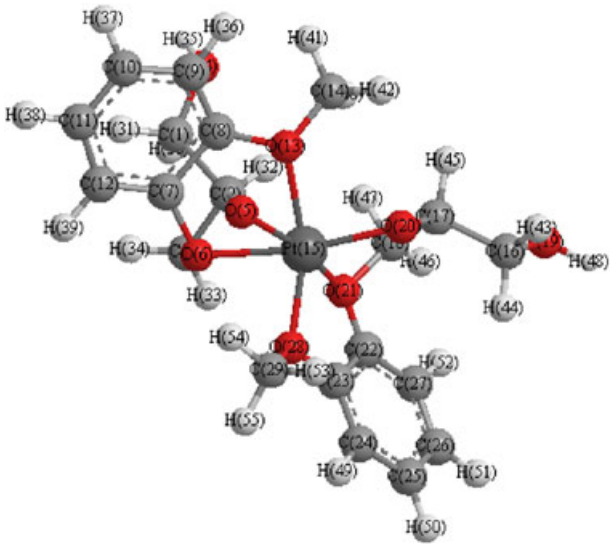

FIGURE 2 Molecular structure of Pt(II) complex **1**

3.6 | Mass spectra

MS is a useful technique to interpret the stoichiometric composition of ligands and complexes. The mass spectrum of the Pt(II) complex **1** was recorded at ambient temperature. The electron impact mass spectrum of the $[Pt(GFS)_2]\cdot 3H_2O$ complex shows a molecular ion peak at m/z = 647.90 amu (calcd = 643 amu). The proposed formula is confirmed also by the appearance of a peak at 198.26 amu corresponding to the GFS ligand moiety ($(C_{10}H_{14}O_4$, atomic mass 198.216 amu). The observed peaks are in good agreement with the proposed formula as indicated by the microanalytical data.[21,36]

3.7 | Powder XRD

The XRD patterns for the Pt(II) chelates **1**–**3** show the crystalline nature of complex **1**, and the amorphous nature of complexes **2** and **3**. This can confirm that the presence of metal ion changes the XRD pattern of the free GFS ligand. Therefore, the non-similarity of the XRD patterns suggests that these chelates have phase structures different from those of the GFS, glycine and 1,10-phenanthroline free ligands.[29,37]

TABLE 1 Selected geometric parameters for Pt(II) complex **1**

Bond length (Å)		Bond angle (°)	
C(29)–H(55)	1.116	H(48)–O(19)–C(16)	109.109
C(29)–H(54)	1.113	H(44)–C(16)–H(43)	107.845
C(29)–H(53)	1.116	H(44)–C(16)–O(19)	107.703
C(27)–H(52)	1.1	H(44)–C(16)–C(17)	112.723
C(26)–H(51)	1.103	H(43)–C(16)–O(19)	107.017
C(25)–H(50)	1.103	H(43)–C(16)–C(17)	110.93
C(24)–H(49)	1.101	O(19)–C(16)–C(17)	110.393
O(19)–H(48)	0.96	H(45)–C(17)–O(20)	108.88
C(18)–H(47)	1.119	H(45)–C(17)–C(18)	109.531
C(18)–H(46)	1.109	H(45)–C(17)–C(16)	105.909
C(17)–H(45)	1.119	O(20)–C(17)–C(18)	109.186
C(16)–H(44)	1.11	O(20)–C(17)–C(16)	108.361
C(16)–H(43)	1.114	C(18)–C(17)–C(16)	114.807
C(14)–H(42)	1.116	H(35)–O(4)–C(1)	108.727
C(14)–H(41)	1.11	H(31)–C(1)–H(30)	100.603
C(14)–H(40)	1.113	H(31)–C(1)–O(4)	106.415
C(12)–H(39)	1.101	H(31)–C(1)–C(2)	121.269
C(11)–H(38)	1.104	H(30)–C(1)–O(4)	102.101
C(10)–H(37)	1.104	H(30)–C(1)–C(2)	108.31
C(9)–H(36)	1.1	O(4)–C(1)–C(2)	115.473
O(4)–H(35)	0.959	H(32)–C(2)–O(5)	132.115
C(3)–H(34)	1.115	H(32)–C(2)–C(3)	112.904
C(3)–H(33)	1.113	H(32)–C(2)–C(1)	76.938
C(2)–H(32)	1.192	O(5)–C(2)–C(3)	106.382
C(1)–H(31)	1.11	O(5)–C(2)–C(1)	128.607
C(1)–H(30)	1.123	C(3)–C(2)–C(1)	91.943
O(28)–Pt(15)	1.948	H(55)–C(29)–H(54)	101.768
O(6)–Pt(15)	2.085	H(55)–C(29)–H(53)	109.69
O(13)–Pt(15)	2.065	H(55)–C(29)–O(28)	111.65
O(5)–Pt(15)	1.859	H(54)–C(29)–H(53)	106.581
O(21)–Pt(15)	1.945	H(54)–C(29)–O(28)	113.972
O(20)–Pt(15)	1.945	H(53)–C(29)–O(28)	112.542
C(18)–O(21)	1.432	H(51)–C(26)–C(27)	120.575
C(23)–O(28)	1.239	H(51)–C(26)–C(25)	120.002
O(28)–C(29)	1.439	C(27)–C(26)–C(25)	119.423
O(21)–C(22)	1.24	H(50)–C(25)–C(26)	120.002
C(22)–C(27)	1.35	H(50)–C(25)–C(24)	120.595
C(26)–C(27)	1.34	C(26)–C(25)–C(24)	119.402
C(25)–C(26)	1.337	H(52)–C(27)–C(22)	123.072
C(24)–C(25)	1.34	H(52)–C(27)–C(26)	115.097
C(23)–C(24)	1.351	C(22)–C(27)–C(26)	121.824
C(22)–C(23)	1.352	H(49)–C(24)–C(25)	115.302
C(17)–O(20)	1.406	H(49)–C(24)–C(23)	122.971
C(16)–O(19)	1.413	C(25)–C(24)–C(23)	121.724
C(17)–C(18)	1.533	O(28)–C(23)–C(24)	125.05
C(16)–C(17)	1.523	O(28)–C(23)–C(22)	116.036
C(3)–O(6)	1.36	C(24)–C(23)–C(22)	118.901
C(8)–O(13)	1.413	H(47)–C(18)–H(46)	99.874
O(13)–C(14)	1.441	H(47)–C(18)–O(21)	110.564
O(6)–C(7)	1.455	H(47)–C(18)–C(17)	109.968
C(7)–C(12)	1.342	H(46)–C(18)–O(21)	115.968
C(11)–C(12)	1.343	H(46)–C(18)–C(17)	113.542
C(10)–C(11)	1.345	O(21)–C(18)–C(17)	106.783
C(9)–C(10)	1.344	O(21)–C(22)–C(27)	125.249
C(8)–C(9)	1.346	O(21)–C(22)–C(23)	116.036
C(7)–C(8)	1.538	C(27)–C(22)–C(23)	118.708
C(2)–O(5)	1.972	Pt(15)–O(28)–C(23)	109.248
C(1)–O(4)	1.42	Pt(15)–O(28)–C(29)	118.981
C(2)–C(3)	1.495	C(23)–O(28)–C(29)	117.743
C(1)–C(2)	1.699	Pt(15)–O(21)–C(18)	107.882
		Pt(15)–O(21)–C(22)	109.546
		C(18)–O(21)–C(22)	117.619
		Pt(15)–O(20)–C(17)	114.078
		H(42)–C(14)–H(41)	104.479
		H(42)–C(14)–H(40)	107.289
		H(42)–C(14)–O(13)	111.942
		H(41)–C(14)–H(40)	105.253
		H(41)–C(14)–O(13)	113.964
		H(40)–C(14)–O(13)	113.226
		Pt(15)–O(5)–C(2)	61.95
		O(28)–Pt(15)–O(6)	78.769
		O(28)–Pt(15)–O(13)	152.402
		O(28)–Pt(15)–O(5)	100.558
		O(28)–Pt(15)–O(21)	77.626
		O(28)–Pt(15)–O(20)	109.623
		O(6)–Pt(15)–O(13)	82.541
		O(6)–Pt(15)–O(5)	48.466
		O(6)–Pt(15)–O(21)	113.66
		O(6)–Pt(15)–O(20)	166.883
		O(13)–Pt(15)–O(5)	51.957
		O(13)–Pt(15)–O(21)	128.949
		O(13)–Pt(15)–O(20)	85.916
		O(5)–Pt(15)–O(21)	161.397
		O(5)–Pt(15)–O(20)	118.839
		O(21)–Pt(15)–O(20)	78.57
		H(34)–C(3)–H(33)	108.198
		H(34)–C(3)–O(6)	110.36
		H(34)–C(3)–C(2)	123.38
		H(33)–C(3)–O(6)	117.04
		H(33)–C(3)–C(2)	123.936
		O(6)–C(3)–C(2)	65.797
		H(38)–C(11)–C(12)	118.625
		H(38)–C(11)–C(10)	119.022
		C(12)–C(11)–C(10)	122.345
		H(37)–C(10)–C(11)	118.295
		H(37)–C(10)–C(9)	118.386
		C(11)–C(10)–C(9)	123.271
		Pt(15)–O(13)–C(8)	114.04
		Pt(15)–O(13)–C(14)	123.58
		C(8)–O(13)–C(14)	118.82
		H(36)–C(9)–C(10)	118.428
		H(36)–C(9)–C(8)	121.56

(*Continues*)

(*Continues*)

TABLE 1 (Continued)

Bond length (Å)	Bond angle (°)	
	C(10)–C(9)–C(8)	119.989
	H(39)–C(12)–C(7)	120.314
	H(39)–C(12)–C(11)	121.456
	C(7)–C(12)–C(11)	118.229
	Pt(15)–O(6)–C(3)	96.571
	Pt(15)–O(6)–C(7)	112.873
	C(3)–O(6)–C(7)	104.155
	O(13)–C(8)–C(9)	127.976
	O(13)–C(8)–C(7)	115.865
	C(9)–C(8)–C(7)	115.85
	O(6)–C(7)–C(12)	126.131
	O(6)–C(7)–C(8)	113.566
	C(12)–C(7)–C(8)	120.242

3.8 | Thermal analysis of metal complexes

The thermal stabilities of GFS and its metal complexes (**1**, **2** and **3**) were investigated using TG and DTG with a heating rate of 10°C min^{-1} from 30 to 1000°C to get information about the thermal decomposition behaviour of these new complexes. The TG and DTG data are summarized in Table 3. The weight losses for each metal complex were calculated within the corresponding temperature ranges.

The thermogram of the binary complex **1** shows three steps of decomposition. The first step of decomposition occurs in the range 45–130°C, corresponding to the loss of three hydrated water molecules, and is accompanied by a weight loss of 7.86% (calcd 8.40%). The second and third stages of decomposition involve the removal of $C_{20}H_{26}O_8$ molecule in the range 130–500°C, and are accompanied by a weight loss of 61.92% (calcd 61.28%). The total weight loss amounts to 69.68% (calcd 69.78%) leaving platinum as a residue.

The thermogram of the ternary complex **2** shows four steps of decomposition. The first and second stages of decomposition occur in the range 30–305°C, corresponding to the loss of $2H_2O$ and $C_8H_{16}ClO$ molecules and are accompanied by a weight loss of 27.98% (calcd 28.00%). The third and fourth stages of decomposition involve the removal of $C_{12}H_{16}NO_9$ molecule in the range 305–995°C, and are accompanied by a weight loss of 44.06% (calcd 44.63%). The total weight loss amounts to 72.04% (calcd 72.63%) leaving platinum as a residue.

The thermogram of the ternary complex **3** shows three steps of decomposition. The first and second stages of decomposition occur in the range 30–335°C, corresponding to the loss of $C_{20}H_{15}ClO_5$ molecule, and are accompanied by a weight loss of 43.80% (calcd 44.00%). The third stage of decomposition involves the removal of $C_{12}H_{21}ClN_2O_3$ molecule in the range 335–615°C, and is accompanied by a weight loss of 31.10% (calcd 32.80%). The total weight loss amounts to 75.00% (calcd 76.80%) leaving platinum as a residue.

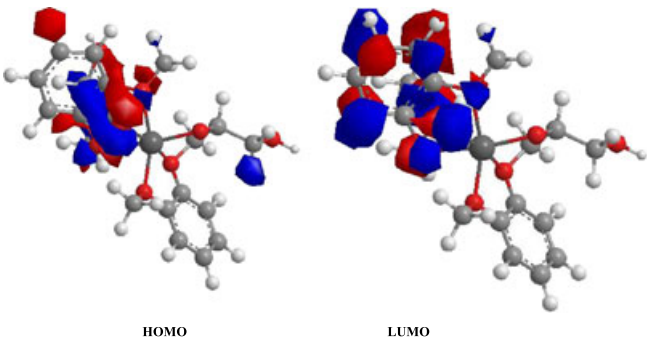

FIGURE 3 HOMO and LUMO of Pt(II) complex **1**

3.9 | Structural interpretation

The structures of the binary and ternary complexes of GFS with Pt(II) ion were confirmed from elemental analyses, IR, ^1H NMR and UV–visible spectra, molar conductance, solid reflectance, XRD and thermal analyses (TG and DTG).[20,21,29,30] The proposed structural formulas of the complexes are summarized as three types of coordination as shown in Figure 4.

3.10 | Antimicrobial studies

GFS drug and the newly synthesized Pt(II) complexes **1–3** were screened for their antibacterial activity against two Gram-positive bacteria (*Bacillus subtilis* and *Staphylococcus aureus*) and two Gram-negative bacteria (*Neisseria gonorrhoeae* and *Escherichia coli*) and for their antifungal activity against *Candida albicans* using the diffusion agar technique.[38,39] All the compounds were placed at four equidistant places at a distance of 2 cm from the centre in inoculated Petri plates. DMSO served as control, while amikacin and ketokonazole were used as standard drugs. All determinations were made in triplicate for each of the compounds. Average of three independent readings for each compound was recorded. The Petri plates were kept in a refrigerator for 24 h for prediffusion. Finally the Petri plates were incubated at 30°C for 24 h. The bacterial growth inhibitory capacities of the ligand and its complexes (Table 4) follow the order:

for *B. subtilis*: GFS = 0 < amikacin <**1** = **2** < **3**
for *E. coli*: GFS = 0 < amikacin <**2** < **1** < **3**
for *N. gonorrhoeae*: GFS = 0 < amikacin <**2** < **1** < **3**
for *S. aureus*: GFS = 0 < amikacin <**1** < **2** < **3**

TABLE 2 Calculated quantum chemical parameters for Pt(II) complex **1**

E_{HOMO} (eV)	E_{LUMO} (eV)	ΔE (eV)	χ (eV)	η (eV)	σ (eV^{-1})	*Pi* (eV)	*S* (eV^{-1})	ω (eV)	ΔN_{max}
−4.39	−1.842	2.548	3.116	1.274	0.785	−3.116	0.393	3.811	2.446

TABLE 3 Thermoanalytical results (TG and DTG) for GFS and its binary and ternary Pt(II) metal complexes

Compound	DTA peak (°C)	TG range (°C)	T_s (°C)	n^a	Mass loss (%)		Total mass loss (%), found (calcd)	Assignment	Residue
					Found	Calcd			
1	110(−), 274(+), 444(−)	45–130, 130–500	95, 222, 430	12	7.8661.92	8.4061.28	69.68 (69.78)	Loss of $3H_2O$Loss of $C_{20}H_{26}O_8$	Pt
2	40(−), 153(+), 254(−), 299(−), 411(+), 520(+)	30–305, 305–995	36, 303, 350, 508	22	27.9844.06	28.0044.63	72.04 (72.63)	Loss of $2H_2O$ and $C_8H_{16}ClO$ Loss of $C_{12}H_{16}NO_9$	Pt
3	113(−), 217(+), 449(+)	30–335, 335–615	182, 235, 450	21	43.8031.10	44.0032.80	75.00 (76.80)	Loss of $C_{20}H_{15}ClO_5$ Loss of $C_{12}H_{21}ClN_2O_3$	Pt

[a]Number of decomposition steps.

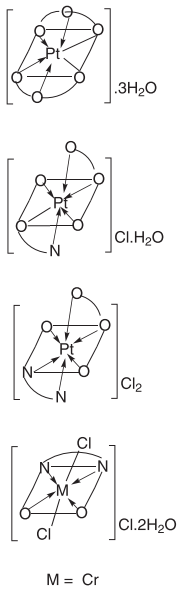

FIGURE 4 Structures of complexes **1–3**

The Pt(II) complex **3** shows greater antibacterial activity (Table 4 and Figure 5) while Pt(II) complex **2** shows lower antibacterial activity. The variation in the activity of the metal complexes against different organisms depends on the impermeability of the microorganism cells or on differences in ribosome of microbial cells.[40] The Pt(II) complexes **1–3** show the best growth inhibition with inhibition zone diameter ranging from 10.0 to 31.0 mm indicating that the coordination of Pt(II) ion to the GFS ligand enhances the antimicrobial activity. Pt(II) complexes **1** and **2** show no antifungal activity against *C. albicans* while complex **3** has a marked antifungal activity. The activities of GFS ligand and its metal complexes were confirmed by calculating the activity index according to the following relation:[6,30,41]

$$\text{Activity index } (A) = \frac{\text{Inhibition zone of compound (mm)}}{\text{Inhibition zone of standard drug (mm)}} \times 100$$

From the data, it is concluded that complex **3** has the highest activity index followed by complex **1**, while complex **2** has the lowest activity index.

3.11 | Anticancer activity

In recent years, there has been a rapid expansion in research and development of new metal-based anticancer drugs to improve clinical effectiveness, reduce general toxicity and broaden the spectrum of activity. Chemical, pharmacological and clinical research on anticancer coordination complexes has yielded remarkable anticancer agents such as cisplatin, carboplatin and oxaliplatin. The foremost target of most research groups was to find a convenient anticancer drug that can be used efficiently for the treatment of human tumours. The inclusion of biologically active ligands into organometallic complexes offers much scope for the design of novel drugs with enhanced, targeted activity. Studies of

TABLE 4 Antimicrobial activity of GFS drug and its Pt(II) complexes **1–3**

Sample	Inhibition zone diameter (mm per mg sample) (Activity index, %)				
	Bacillus subtilis	*Escherichia coli*	*Neisseria gonorrhoeae*	*Staphylococcus aureus*	*Candida albicans*
Control: DMSO	0	0	0	0	0
Amikacin	6	9	7	6	0
Ketokonazole	—	—	—	—	9
GFS	0	0	0	0	0
HGly	9	9	9	9	0
1,10-Phen	38	28	36	48	35
1	12 (200)	11 (122.2)	12 (171.4)	11 (183.3)	0
2	10 (166.7)	10 (111.1)	11 (157.1)	11 (183.3)	0
3	31 (516.7)	26 (288.9)	28 (400)	22 (366.7)	16 (177.8)

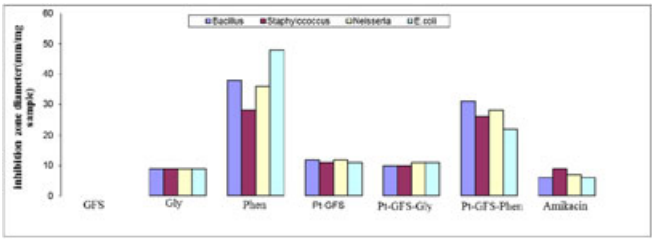

FIGURE 5 Antimicrobial activity of GFS, HGly, Phen and Pt(II) complexes **1–3**

GFS drug and its binary and ternary Pt(II) metal complexes **1–3** were evaluated for their activity against breast cancer cell line (MCF7) by using 100 μg ml^{-1} drug or metal complex concentration. From the results, it is clear that complexes **1** and **2** are moderately active against breast cancer cells with inhibition ratio of 80%, while the ternary complex **3** utilized in this work is markedly active (86% inhibition) against breast cancer cells. It is clear that a pattern of activity can be determined using different drug concentrations (Table 5 and Figure 6). The IC_{50} values are

TABLE 5 Anticancer activity of GFS and its Pt(II) complexes **1–3**

Complex	Surviving fraction (MCF7)					IC_{50} (μg ml^{-1})
	0.0 μg ml^{-1}	5 μg ml^{-1}	12.5 μg ml^{-1}	25 μg ml^{-1}	50 μg ml^{-1}	
GFS	1	0.843	0.594	0.295	0.130	16.6
HGly	1	1	1	1	1	0
1,10-Phen	1	0.482	0.318	0.315	0.297	4.73
1	1	0.914	0.558	0.286	0.219	15.1
2	1	0.877	0.487	0.327	0.154	12.2
3	1	0.236	0.210	0.197	0.299	3.38

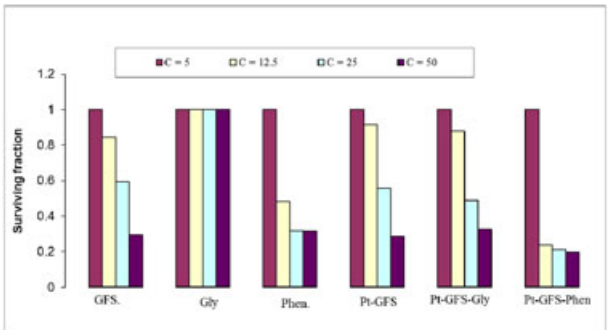

FIGURE 6 Anticancer activity of GFS, HGly, Phen and Pt(II) complexes **1–3** against breast cell line (MCF 7)

such complexes are expected to indicate that new mechanisms of action are possible through combining the bioactivity of a ligand with the properties inherent to a metal, leading to the possibility of overcoming current drug resistance pathways.[6,42]

found to be 15.1, 12.2 and 3.38 μg ml^{-1} for complexes **1**, **2** and **3**, respectively. It is found that the ternary complex **3** has an outstanding IC_{50} value and a very low concentration of this complex can be used to produce 50% inhibition of cell growth.[5,24,30]

4 | CONCLUSIONS

Various physicochemical, spectroscopic and thermal methods of analysis were utilized to characterize the ligand under investigation and its Pt(II) binary and ternary metal chelates in addition to studying their biological and anticancer activities. The cytotoxic activity shown by these metal complexes against MCF7 cell line indicated that chelation of GFS to Pt (II) metal ion resulted in metallic complexes with important biological properties and marked cytotoxic activity, displaying IC_{50} values in a better range than those of many

anti-tumour drugs. Thus, these complexes can be considered as agents with potential anti-tumour activity and can therefore be candidates for further stages of screening *in vitro* and/or *in vivo*.

REFERENCES

[1] http://en.wikipedia.org/wiki/Chemical_biology#Metal_complexes_in_medicine.

[2] R. A. Sánchezdelgado, A. Anzellotti, *Mini-Rev. Med. Chem.* **2004**, *4*, 23.

[3] S. B. Pawar, S. S. Vetal, U. D. Gharate, S. B. Bhawar, *J. Ind. Drugs* **2012**, *49*, 5.

[4] C. Marzano, M. Pellei, F. Tisato, C. Santini, *Anti-Cancer Agents Med. Chem.* **2009**, *9*, 185.

[5] S. M. Emam, I. E. T. El Sayed, N. Nassar, *Spectrochim. Acta A* **2015**, *138*, 942.

[6] A. S. Abu-Surrah, H. H. Al-Sa'doni, M. Y. Abdalla, *Cancer Therapy* **2008**, *6*, 1.

[7] http://en.wikipedia.org/wiki/Guaifenesin.

[8] http://www.fibrokur.com/P333/.

[9] A. A. Bredikhin, A. T. Gubaidullin, Z. A. Bredikhina, D. B. Krivolapov, A. V. Pashagin, I. A. Litvinov, *J. Mol. Struct.* **2009**, *920*, 377.

[10] http://www.webmd.com/drugs/mono-630UAIFENESIN+SUSTAINED-RELEASE+-+ORAL.aspx?drugid=3350&drugname=Guaifenesin+Oral.

[11] A. Z. El-Sonbati, M. A. Diab, A. A. El-Bindary, A. M. Eldesoky, S. M. Morgan, *Spectrochim. Acta A* **2015**, *135*, 774.

[12] A. A. El-Bindary, A. Z. El-Sonbati, M. A. Diab, S. M. Morgan, *J. Mol. Liq.* **2015**, *201*, 36.

[13] A. Albert, *Selective Toxicity*, 6th ed., Wiley, New York **1979**.

[14] S. Chandra, D. Jain, A. K. Sharma, P. Sharma, *Molecules* **2009**, *14*, 174.

[15] P. Skehan, R. Storeng, *J. Natl. Cancer Inst.* **1990**, *42*, 1107.

[16] W. M. I. Hassan, M. A. Badawy, G. G. Mohamed, H. Moustafa, S. Elramly, *Spectrochim. Acta A* **2013**, *111*, 169.

[17] S. Chandra, L. K. Gupta, *Spectrochim. Acta A* **2005**, *61*, 269.

[18] M. A. El-Ghamry, A. A. Saleh, S. M. E. Khalil, A. A. Mohammed, *Spectrochim. Acta A* **2013**, *110*, 205.

[19] W. H. Mahmoud, N. F. Mahmoud, G. G. Mohamed, A. A. El-Bindary, A. Z. El-Sonbati, *J. Mol. Struct.* **2015**, *1086*, 266.

[20] W. H. Mahmoud, N. F. Mahmoud, G. G. Mohamed, A. Z. El-Sonbati, A. A. El-Bindary, *J. Mol. Struct.* **2015**, *1095*, 15.

[21] W. J. Geary, *Coord. Chem. Rev.* **1971**, *7*, 81.

[22] V. L. Dorofeev, *Pharm. Chem. J.* **2004**, *38*, 45.

[23] L. J. Bellamy, *The Infrared Spectra of Complex Molecules*, 3rd ed., Chapman and Hall, London **1975**.

[24] H. F. Abd El-Halim, G. G. Mohamed, M. M. I. El-Dessouky, W. H. Mahmoud, *Spectrochim. Acta A* **2011**, *82*, 8.

[25] C. S. Dilip, V. S. Kumar, S. J. Venison, I. V. Potheher, D. R. Subahashini, *J. Mol. Struct.* **2013**, *1040*, 192.

[26] M. Shebl, H. S. Seleem, B. A. El-Shetary, *Spectrochim. Acta A* **2010**, *75*, 428.

[27] V. P. Singh, S. Singh, D. P. Singh, K. Tiwari, M. Mishra, *J. Mol. Struct.* **2014**, *1058*, 71.

[28] A. A. El-Bindary, G. G. Mohamed, A. Z. El-Sonbati, M. A. Diab, W. M. I. Hassan, S. M. Morgan, A. K. Elkholy, *J. Mol. Liq.* **2016**, *218*, 138.

[29] W. H. Mahmoud, R. G. Deghadi, G. G. Mohamed, *Appl. Organometal. Chem.* **2016**, *30*, 221.

[30] W. H. Mahmoud, M. M. Omar, F. N. Sayed, *J. Therm. Anal. Calorim.* **2016**, *124*, 1071.

[31] S. Madhupriya, K. P. Elango, *Spectrochim. Acta A* **2014**, *118*, 337.

[32] G. G. Mohamed, M. M. Omar, A. A. Ibrahim, *Eur. J. Med. Chem.* **2009**, *44*, 4801.

[33] M. L. Sundararajan, J. Anandakumaran, T. Jeyakumar, *Spectrochim. Acta A* **2014**, *125*, 104.

[34] E. R. Krishna, P. M. Reddy, M. Sarangapani, G. Hanmanthu, B. Geeta, K. S. Rani, V. Ravinder, *Spectrochim. Acta A* **2012**, *97*, 189.

[35] A. Z. El-Sonbati, G. G. Mohamed, A. A. El-Bindary, W. M. I. Hassan, A. K. Elkholy, *J. Mol. Liq.* **2015**, *209*, 625.

[36] C. J. Dhanaraj, J. Johnson, *Spectrochim. Acta A* **2014**, *118*, 624.

[37] J. R. Anacona, J. L. Rodriguez, J. Camus, *Spectrochim. Acta A* **2014**, *129*, 96.

[38] A. W. Bauer, W. M. Kirby, C. Sherris, M. Turck, *Am. J. Clin. Pathol.* **1966**, *45*, 493.

[39] a) B. G. Tweedy, *Phytopathology* **1964**, *55*, 910. (b) S. K. Sengupta, O. P. Pandey, B. K. Srivastava, V. K. Sharma, *Transition Met. Chem.* **1998**, *23*, 349.

[40] S. Gopalakrishnan, R. Rajameena, E. Vadivel, *Int. J. Pharm. Sci. Drug Res.* **2012**, *4*, 31.

[41] L. H. Abdel-Rahman, A. M. Abu-Dief, N. A. Hashem, A. A. Seleem, *Int. J. Nano Chem.* **2015**, *1*, 79.

[42] M. Hanif, Z. H. Chohan, *Spectrochim. Acta A* **2013**, *104*, 468.

How to cite this article: Mahmoud, W. H., Mohamed, G. G., and Mahmoud, N. F. (2016), New bioactive Pt(II) binary and ternary metal complexes with guaifenesin drug: Synthesis, geometrical structure, and spectroscopic and thermal characterization, *Appl. Organometal. Chem.*, doi: 10.1002/aoc.3583